

UNIVERSIDAD SAN FRANCISCO DE QUITO USFQ

Colegio de Posgrados

**On the separation of the information content of the Fermi and Coulomb holes
and their influence on the electronic properties of molecular systems**

Marcos Vinicio Becerra Puebla

**Luis Rincón, Ph.D.
Director de Trabajo de Titulación**

Trabajo de titulación de posgrado presentado como requisito
para la obtención del título de Máster en Química

Quito, 05 de diciembre de 2018

UNIVERSIDAD SAN FRANCISCO DE QUITO USFQ

COLEGIO DE POSGRADOS

HOJA DE APROBACIÓN DE TRABAJO DE TITULACIÓN

**On the separation of the information content of the Fermi and Coulomb holes
and their influence on the electronic properties of molecular systems**

Marcos Vinicio Becerra Puebla

Firmas

Luis Rincón, Ph.D.

Director del Trabajo de Titulación

F. Javier Torres, Ph.D.

Director del Programa de Maestría en
Química

Cesar Zambrano, Ph.D.

Decano del Politécnico

Hugo Burgos, Ph.D.

Decano del Colegio de Posgrados

Quito, 05 de diciembre de 2018

© Derechos de Autor

Por medio del presente documento certifico que he leído todas las Políticas y Manuales de la Universidad San Francisco de Quito USFQ, incluyendo la Política de Propiedad Intelectual USFQ, y estoy de acuerdo con su contenido, por lo que los derechos de propiedad intelectual del presente trabajo quedan sujetos a lo dispuesto en esas Políticas.

Asimismo, autorizo a la USFQ para que realice la digitalización y publicación de este trabajo en el repositorio virtual, de conformidad a lo dispuesto en el Art. 144 de la Ley Orgánica de Educación Superior.

Firma del estudiante:

Nombre:

Marcos Vinicio Becerra Puebla

Código de estudiante:

00140984

C. I.:

2000068052

Lugar, Fecha

Quito, 05 de diciembre de 2018

DEDICATORIA

Dedico este trabajo a mis padres, Teresa y Homero, gracias a su incondicional apoyo para ayudarme a realizar todos mis proyectos.

AGRADECIMIENTOS

Gracias a mis padres, Teresa y Homero, por apoyarme en cada decisión y proyecto de mi vida. Gracias por creer en mí, aconsejarme, ayudarme y por permitirme vivir y disfrutar cada día al máximo cada día.

Gracias al grupo de Química Computacional y Teórica (QCT) de la Universidad San Francisco de Quito, en especial a Javier Torres. Gracias por haber confiado en mí y haberme traído a este grupo hace ya ocho años, nunca olvidaré todas tus enseñanzas a través de este tiempo. Este grupo ha sido como una segunda universidad, donde he aprendido a desarrollarme como un investigador y como persona. Así mismo quiero agradecer de manera especial a Luis Rincón, mi tutor de tesis. Siempre por tenerme paciencia para enseñarme y ayudarme en todo momento. Igualmente, a todos los profesores que forman y formaron parte del grupo, José Mora, Miguel Ángel Méndez, Eduardo Ludeña, y muchos más, que al paso del tiempo he tenido el honor de trabajar con ellos y aprender muchas cosas.

RESUMEN

En este artículo, se utilizan dos funciones de la teoría de la información como una medida de los huecos de Fermi y Coulomb para electrones del mismo espín. El primero es el contenido de la información del hueco de Intercambio–Correlación (χ_{XC}), calculado con la divergencia de Kullback–Leibler usando la densidad de pares condicional respecto a la probabilidad marginal. Como se reportó previamente, el χ_{XC} se puede utilizar para mostrar las regiones en el espacio asociadas al modelo clásico del par de electrones. En este, funciones de onda correlacionadas, tales como CISD, MP2 y CCSD, son consideradas para el cálculo del χ_{XC} . Esto se consigue introduciendo un método de aproximación basado en el uso de los orbitales naturales y sus ocupaciones. Adicionalmente al χ_{XC} , en este trabajo se propone una medida del contenido de la información de la correlación debido a electrones del mismo espín, el cual se calcula en términos de la divergencia de Kullback–Leibler usando una densidad de pares condicional del mismo espín con respecto a la densidad de pares sin correlación de Hartree–Fock (χ_c). La metodología propuesta se discute con los resultados encontrados para átomos de gas noble, la molécula de F_2 y sistemas con enlaces no covalentes.

Palabras clave: Localización electrónica, hueco de Fermi, hueco de Coulomb, correlación electrónica, divergencia de Kullback–Leibler

ABSTRACT

In this paper, two information-based functions are employed as a real space measure of the Fermi and Coulomb holes for same-spin electrons. The first one is the information content of the Exchange-Correlation hole, calculated from the Kullback–Leibler divergence of the same-spin conditional pair density respect to the marginal probability (χ_{XC}). As reported previously, χ_{XC} , can be used to reveal the regions of the space associated to the classical electron pair model. Here, correlated wave-functions, such as CISD, MP2, and CCSD, are considered for the calculation of χ_{XC} . This is achieved by introducing an approximated method based on employing natural orbitals and their occupancy numbers. In addition to χ_{XC} , in this work we propose a measure of the information content of the same-spin correlation hole, which is computed in terms of the Kullback–Leibler divergence of a correlated same-spin conditional pair density respect to the uncorrelated Hartree–Fock pair density (χ_C). The proposed methodology is discussed in the light of the result derived from noble gas atoms, the F_2 molecule and some non-covalently bonded systems.

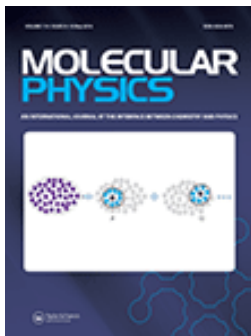
Keywords: Electron localization; Fermi hole; Coulomb hole; electron correlation; Kullback–Leibler divergence.

TABLA DE CONTENIDO

Abstract	11
1. Introduction.....	11
2. The information content of the exchange-correlation hole	12
2.1. The pair density	12
2.2. Kullback–Leibler divergence of the conditional pair density	14
2.3. Approximated pair-density expression from the natural orbitals	15
2.4. The information content of the coulomb hole	16
3. Computational details	17
4. Results and discussion.....	18
4.1. Noble gases	18
4.2. The F ₂ molecule	19
4.3. Non-covalent interactions from the information content of the Coulomb hole.....	21
5. Summary and final remarks	23

ÍNDICE DE FIGURAS

- Figure 1. Plots Of χ_{XC} at the RHF and CISD and χ_C for CISD as a function of the distance to the nuclei for the case of noble gas atoms: (A) Ne and (B) Ar 19
- Figure 2. Plots of χ_{XC} and χ_C along the bond axis of the F_2 molecule. At $R(F-F)= 1.4 \text{ \AA}$; and at $R(F-F)= 2.0 \text{ \AA}$. With levels of theory: RHF, CISD, MP2 and CCSD..... 19
- Figure 3. (a) χ_{XC} and (b) χ_C for the water dimer 20
- Figure 4. χ_C for the hydrogen fluoride clusters from the dimer to the hexamer. A plot of the Binding Energy per Hydrogen Bond versus the maxima of χ_C at the hydrogen border..... 22
- Figure 5. χ_{XC} and χ_C for the benzene dimer T-shape..... 22



Molecular Physics

An International Journal at the Interface Between Chemistry and Physics

ISSN: 0026-8976 (Print) 1362-3028 (Online) Journal homepage: <http://www.tandfonline.com/loi/tmph20>

On the separation of the information content of the Fermi and Coulomb holes and their influence on the electronic properties of molecular systems

Luis Rincon, F. Javier Torres, Marcos Becerra, Shubin Liu, Alain Fritsch & Rafael Almeida

To cite this article: Luis Rincon, F. Javier Torres, Marcos Becerra, Shubin Liu, Alain Fritsch & Rafael Almeida (2018): On the separation of the information content of the Fermi and Coulomb holes and their influence on the electronic properties of molecular systems, Molecular Physics, DOI: [10.1080/00268976.2018.1530462](https://doi.org/10.1080/00268976.2018.1530462)

To link to this article: <https://doi.org/10.1080/00268976.2018.1530462>



Published online: 08 Oct 2018.



Submit your article to this journal [↗](#)



Article views: 31



View Crossmark data [↗](#)

RESEARCH ARTICLE



On the separation of the information content of the Fermi and Coulomb holes and their influence on the electronic properties of molecular systems

Luis Rincon^{a,b}, F. Javier Torres^a, Marcos Becerra^a, Shubin Liu^c, Alain Fritsch^d and Rafael Almeida^b

^aGrupo de Química Computacional y Teórica (QCT-USFQ) and Instituto de Simulación Computacional (ISC-USFQ), Dept. de Ingeniería Química, Colegio de Ciencias e Ingeniería, Universidad San Francisco de Quito, Quito, Ecuador; ^bDepartamento de Química, Facultad de Ciencias, Universidad de Los Andes (ULA), Mérida, Venezuela; ^cResearch Computing Center, University of North Carolina, Chapel Hill, NC, USA; ^dInstitut des Sciences Moléculaires, Theoretical Chemistry & Modeling Group, Université Bordeaux, Talence, France

ABSTRACT

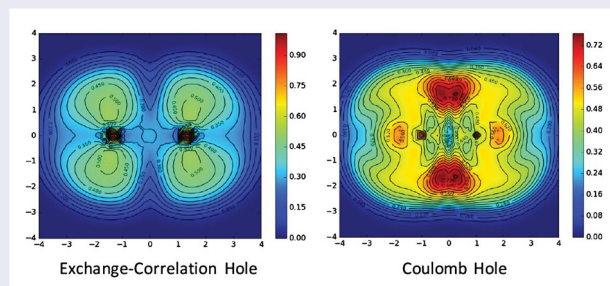
In this paper, two information-based functions are employed as a real space measure of the Fermi and Coulomb holes for *same-spin* electrons. The first one is the information content of the Exchange–Correlation hole, calculated from the Kullback–Leibler divergence of the *same-spin* conditional pair density respect to the marginal probability (χ_{XC}). As reported previously, χ_{XC} can be used to reveal the regions of the space associated to the classical electron pair model. Here, correlated wave-functions, such as CISD, MP2, and CCSD, are considered for the calculation of χ_{XC} . This is achieved by introducing an approximated method based on employing natural orbitals and their occupancy numbers. In addition to χ_{XC} , in this work we propose a measure of the information content of the *same-spin* correlation hole, which is computed in terms of the Kullback–Leibler divergence of a correlated *same-spin* conditional pair density respect to the uncorrelated Hartree–Fock pair density (χ_C). The proposed methodology is discussed in the light of the result derived from noble gas atoms, the F_2 molecule and some non-covalently bonded systems.

ARTICLE HISTORY

Received 13 July 2018
Accepted 19 September 2018

KEYWORDS

Electron localisation; Fermi hole; Coulomb hole; electron correlation; Kullback–Leibler divergence



1. Introduction

The electron pair concept has played a fundamental role in the chemical thinking, becoming a part of the chemical intuition, customarily employed in the description and understanding of a variety of molecular properties [1]. One of the challenges of modern theoretical chemistry is to develop a link between the classical *electron pair* concept and the results of sophisticated electronic structure calculations. Nowadays, the most widely used procedure consists in the analysis of the same-spin pair density, Γ ,

or the related same-spin conditional pair density [2–10], γ . In this context, it is important to notice that γ is composed of two non-separable contributions: (i) the Fermi hole, arising from the antisymmetric character of the wave-function, and (ii) the same-spin component of the Coulomb hole, which is a consequence of the electronic repulsion between *same-spin* electrons. Moreover, it is possible to state that the properties of the different types of chemical interactions, ranging from strong covalent bonds to weak dispersion forces, are a consequence of

CONTACT Luis Rincon ✉ Irincon@usfq.edu.ec  Grupo de Química Computacional y Teórica (QCT-USFQ) and Instituto de Simulación Computacional (ISC-USFQ), Dept. de Ingeniería Química, Colegio de Ciencias e Ingeniería, Universidad San Francisco de Quito, Diego de Robles y Via Interoceánica, Quito 17-1200-841, Ecuador

the interplay between the Fermi and the Coulomb holes. Nevertheless, as stated by Lennard-Jones, for most of the interactions, the effect of the former is the predominant one:

Electrons of like spin tend to avoid each other. This effect is more powerful, much more powerful, than the electrostatic forces. It does more to determine the shapes and properties of molecules than other single factor. It is the exclusion principle that plays the dominant role in chemistry. Its all-pervading influence does not seem hitherto to have fully realised by chemists, but it is safe to say that ultimately it will be regarded as the most important property to be learned by those concerned with molecular structure [11].

Due to the importance of these ideas, during the last decades, they have been revisited and extended by many authors [2–10]. As a result, a number of electron localisation measurements based on the analysis of the pair density have been proposed in the last three decades (see for instance [12–23]). In these regards, it has been demonstrated that electron localisation can be revealed using information theoretical tools, and as examples, we can mention the information theoretical electron localisation function (ELF) of Nalewajski *et al.* [24] and our electron localisation measure based on the analysis of the information content of the Exchange-Correlation hole [25, 26]. The last mentioned quantity is capable of revealing electron pair localisation regions in systems with different bond types: covalent, multiple, aromatic, ionic, charge shifting, and three centre-two electron bonds [25, 26]. Nevertheless, in spite of the accuracy achieved in the characterisation of bonding, lone pair and core electron regions, it has not been possible to characterise, with comparable detail, the regions associated with non-classical interactions, i.e. non-covalent bonding. It is important to point out that the electron correlation play an important role in the formation of all these interactions [27, 28]; hence, for properly describing them through the Exchange-Correlation hole analysis is critical to access the Coulomb hole information content, which in good measure, is hindered by the dominant Fermi hole. Thus, it is clear that for gaining further insights on the properties of many molecular systems, some strategies are required to study separately the behaviour of the Fermi and Coulomb holes. In these regards, the objectives of this paper are twofold: The first objective is to extend our recent electron localisation measurement based on the information content of the *same-spin* conditional pair density for the case when correlated wave-functions are used [25, 26]. For this, an approach that makes use of the natural orbitals, and their associated occupancy numbers, while fulfill the Pauli principle requirement and some of the exact

second-order density matrix sum rule is presented. This procedure allows to calculate the *same-spin* conditional pair density from methods such as CISD, MP2 and CCSD. Our second objective is related to the possibility of visualise directly the effect of the Coulomb correlation for *same-spin* electrons in the space. Thus, by comparing the *same-spin* pair density at the correlated and un-correlated levels we introduce an information theoretical measurement of the Coulomb hole that reveals the zones of the space more affected by the electron correlation.

The outline of this paper is as follows: The information-based measurements of the Fermi and Coulomb holes are presented in Section 2. The basic concepts and notations relevant to the *same-spin* pair density function and the associated *same-spin* conditional probability are discussed in the Section 2.1. In Section 2.2, we present our previous information tool based on the information gained by an electron from ‘knowing’ about the position of a reference electron with the same spin is presented on the basis of the Kullback–Leibler divergence between the *same-spin* conditional probability respect to the marginal probability, $D_{KL,XC}$. Moreover, from this result, the information content of the Exchange-Correlation hole is defined through a modified function that is roughly normalised between 0 and 1, χ_{XC} . In Section 2.3, we introduce an approximate procedure that allows the calculation of the *same-spin* pair density for correlated wave-functions from their natural orbitals expansion. In Section 2.4, a new function, χ_C , is introduced, which provides the information gained when the correlated conditional pair density is employed, instead of the Hartree–Fock one. Computational details are presented in Section 3. In Section 4, we present preliminary calculations of χ_{XC} and χ_C to some atomic systems and a series of problems in which mono-determinantal approximations sound problematic. The final remarks are presented in Section 5, making emphasis in a discussion on the challenges that have to be addressed to improve our information-based tools. Finally, we conclude the work by enumerating some problems in which χ_{XC} and χ_C could be of valuable use in the future.

2. The information content of the exchange-correlation hole

2.1. The pair density

We start this section by introducing the concept of the *same-spin* pair density, and the associated *same-spin* conditional pair density, as central quantities for

the following discussion about the Fermi and Coulomb hole.

For a system of N^σ electrons of spin σ , the *same-spin* pair density, $\Gamma^{\sigma\sigma}(\mathbf{r}_1, \mathbf{r}_2)$, is defined as:

$$\Gamma^{\sigma\sigma}(\mathbf{r}_1, \mathbf{r}_2) = \frac{N^\sigma(N^\sigma - 1)}{2} \sum_{\sigma_1} \delta(\sigma_1, \sigma) \sum_{\sigma_2} \delta(\sigma_2, \sigma) \int d\mathbf{x}_3 \cdots \int d\mathbf{x}_N |\Psi(\mathbf{x}_1, \mathbf{x}_2, \dots, \mathbf{x}_N)|^2. \quad (1)$$

Here, $\Psi(\mathbf{x}_1, \mathbf{x}_2, \dots, \mathbf{x}_N)$, denotes an antisymmetric $N = N^\alpha + N^\beta$ electron wavefunction and $\mathbf{x}_i = (\mathbf{r}_i, \sigma_i)$ corresponds to the position and spin coordinates of electron i . $\Gamma^{\sigma\sigma}(\mathbf{r}_1, \mathbf{r}_2)$ is interpreted as $N^\sigma(N^\sigma - 1)/2$ -times the joint probability density to find one electron at \mathbf{r}_1 with spin σ and, simultaneously, a second electron at \mathbf{r}_2 with the same spin.

Some of the properties of $\Gamma^{\sigma\sigma}(\mathbf{r}_1, \mathbf{r}_2)$ are:

- If $\mathbf{r}_1 \neq \mathbf{r}_2$, $\Gamma^{\sigma\sigma}(\mathbf{r}_1, \mathbf{r}_2)$ is always positive:

$$\Gamma^{\sigma\sigma}(\mathbf{r}_1, \mathbf{r}_2) > 0; \quad (2)$$

- It vanishes at electron coalescence due to the Pauli Principle, that is:

$$\Gamma^{\sigma\sigma}(\mathbf{r}_1, \mathbf{r}_1) = 0. \quad (3)$$

- It is normalised to the number of electron pairs of σ spin:

$$\int d\mathbf{r}_1 \int d\mathbf{r}_2 \Gamma^{\sigma\sigma}(\mathbf{r}_1, \mathbf{r}_2) = \frac{N^\sigma(N^\sigma - 1)}{2}. \quad (4)$$

- Integration over the coordinates of electron 2 leads to the σ -spin electron density at \mathbf{r}_1 , $\rho^\sigma(\mathbf{r}_1)$, with a factor of $(N^\sigma - 1)/2$:

$$\int d\mathbf{r}_2 \Gamma^{\sigma\sigma}(\mathbf{r}_1, \mathbf{r}_2) = \frac{(N^\sigma - 1)}{2} \rho^\sigma(\mathbf{r}_1). \quad (5)$$

- When $\Psi(\mathbf{x}_1, \mathbf{x}_2, \dots, \mathbf{x}_N)$ is approximated by a single Slater determinant with a set of ortho-normalised molecular orbitals, $\{\phi_i^\sigma\}$, $\Gamma^{\sigma\sigma}(\mathbf{r}_1, \mathbf{r}_2)$ can be computed as follows:

$$\Gamma^{\sigma\sigma}(\mathbf{r}_1, \mathbf{r}_2) = \frac{1}{2} \times \left(\rho^\sigma(\mathbf{r}_1)\rho^\sigma(\mathbf{r}_2) - \left| \sum_i \phi_i^\sigma(\mathbf{r}_1)\phi_i^\sigma(\mathbf{r}_2) \right|^2 \right). \quad (6)$$

The conditional pair density, $\gamma_{\text{cond}}^{\sigma,\sigma}(\mathbf{r}_2 | \mathbf{r}_1)$, is related to $\Gamma^{\sigma\sigma}(\mathbf{r}_1, \mathbf{r}_2)$ by the equation,

$$\Gamma^{\sigma\sigma}(\mathbf{r}_1, \mathbf{r}_2) = \frac{1}{2} \rho^\sigma(\mathbf{r}_1) \gamma_{\text{cond}}^{\sigma,\sigma}(\mathbf{r}_2 | \mathbf{r}_1). \quad (7)$$

Here, $\gamma_{\text{cond}}^{\sigma,\sigma}(\mathbf{r}_2 | \mathbf{r}_1)$ can be interpreted as the probability density of the $N^\sigma - 1$ electrons at \mathbf{r}_2 when it is known, with certainty, that a reference electron is at position \mathbf{r}_1 . $\gamma_{\text{cond}}^{\sigma,\sigma}(\mathbf{r}_2 | \mathbf{r}_1)$ can be partitioning in two terms: (i) an uncorrelated density-dependent term and (ii) a part containing the exchange-correlation hole density [29–31],

$$\begin{aligned} \gamma_{\text{cond}}^{\sigma,\sigma}(\mathbf{r}_2 | \mathbf{r}_1) &= \rho^\sigma(\mathbf{r}_2)(1 + f_{\text{XC}}^\sigma(\mathbf{r}_2 | \mathbf{r}_1)) \\ &= \rho^\sigma(\mathbf{r}_2) + \rho_{\text{XC}}^\sigma(\mathbf{r}_2 | \mathbf{r}_1). \end{aligned} \quad (8)$$

Conventionally, the exchange-correlation hole density, $\rho_{\text{XC}}^\sigma(\mathbf{r}_2 | \mathbf{r}_1) = \rho^\sigma(\mathbf{r}_2)f_{\text{XC}}^\sigma(\mathbf{r}_2 | \mathbf{r}_1)$, is defined as a negative quantity, and it integrates to minus one electron for any position of the reference electron. Therefore, the presence of an electron at \mathbf{r}_1 reduce the probability of finding an electron at \mathbf{r}_2 with the same spin by a fraction $f_{\text{XC}}^\sigma(\mathbf{r}_2 | \mathbf{r}_1)$ [30]. Moreover, both the conditional pair density and the hole density depend parametrically on the position \mathbf{r}_1 .

In the Hartree–Fock approximation the hole density, $\rho_X^\sigma(\mathbf{r}_2 | \mathbf{r}_1)$, or alternatively the Fermi hole density, only contains exchange effects and is completely determined by the one-electron density matrix. Thus, the Fermi hole is simply interpreted as the exclusion of one electron due to the localisation of another electron with the *same-spin* at some reference position [2–6]. On the other hand, when the electron correlation is explicitly introduced, part of the Coulomb correlation hole is also included in the description of the system. The Coulomb hole is customarily defined as the difference between the exact, or a correlated derived, conditional pair density and the Hartree–Fock one [31], but alternative definitions can be found in the literature [32].

At this point, it is important to emphasise that the *same-spin* conditional pair density can be obtained at any level of theory, as long as its related *same-spin* pair density is also accessible. However, as pointed out by Lennard-Jones, it is well-known that the effect of the antisymmetry in the pair density is the dominant one. As a consequence, the uncorrelated Hartree–Fock model is enough to provide a good qualitative description of the full conditional pair density localisation pattern. In other words, the Coulomb correlation has a comparatively minor effect in the *same-spin* conditional pair density pattern; and therefore, its description constitutes a more challenging task. Thus, in the next sections, the localisation of $\rho_{\text{XC}}^\sigma(\mathbf{r}_2 | \mathbf{r}_1)$ will be discussed, together with the interplay between the Fermi and the Coulomb holes, obtained at various levels of theory.

2.2. Kullback–Leibler divergence of the conditional pair density

The concept of Information was introduced in statistic for the first time by Sir R.A. Fisher in 1925 [33]. Later, in 1948, C.A. Shannon introduced the definition of ‘entropy’ as an information measure in his seminal paper entitled: ‘A mathematical theory of communication’ [34]. In some way, Information Theory, IT, is a convenient way to analyse any probabilistic system of observations. Roughly speaking, whenever we need to make statistical inference, we seek for ‘information’. Thus, IT applications are found in any fields characterised by the use of some kind of *statistical estimation* or *statistical inference*. In this context, IT has been proposed as a tool for the analysis of the electronic structure of atoms, molecules, and solids where, in contrast with classical systems, the dynamics is described in a probabilistic way due to the quantum character of the components [35–43]. In this sense, since the seminal works of Collins and Smith [44] which propose a connection between the correlation energy of a molecular system and an IT measurement (the Jaynes entropy), a number of important contributions have appeared in this field [45–58]. The connection between the IT tools and the electron correlation in atoms and molecules reveals that the essential part of the correlation holes can be captured by entropic measurements.

An important generalisation to the Shannon’s entropy, called the ‘divergence’, also known as the ‘missing information’, or ‘entropy deficiency’, was proposed by Kullback and Leibler in 1951 [59, 60]. For two normalised probability density functions (PDFs), say $p(x)$ and $q(x)$, that depend on the same continuous random variables, ‘the Kullback–Leibler divergence of p respect to q ’ is defined as follows:

$$D_{\text{KL}}(p \parallel q) = \int p(x) \log_2 \frac{p(x)}{q(x)} dx. \quad (9)$$

In this equation, the logarithm is taken in base 2 to compute $D_{\text{KL}}(p \parallel q)$ in units of bits; however, it is important to indicate that most formulas involving $D_{\text{KL}}(p \parallel q)$ hold regardless the base of the logarithm employed. $D_{\text{KL}}(p \parallel q)$ is usually interpreted as the amount of information lost when the PDF q is used to approximate the PDF p . This interpretation is used along the present paper. Moreover, it is found that $D_{\text{KL}}(p \parallel q)$ is always non-negative as a result of the Gibbs’ inequality [61], and it is zero if p and q are the same in the whole domain. It is important to mention that some upper bounds of D_{KL} based on the χ^2 distance have been proposed (see for instance Ref. [62, 63]).

Following our previous work [43], we will assume that electron localisation can be revealed from the information content of the Exchange-Correlation hole. Based on this unorthodox (but measurable) definition of electron localisation, we introduce in 2016 [25] the Kullback–Leibler divergence of the conditional probability density as follows:

$$D_{\text{KL},\text{XC}}(\mathbf{r}_1) = \int d\mathbf{r}_2 \rho_{\text{cond}}^{\sigma,\sigma}(\mathbf{r}_2 \mid \mathbf{r}_1) \log_2 \times \left(\frac{\rho_{\text{cond}}^{\sigma,\sigma}(\mathbf{r}_2 \mid \mathbf{r}_1)}{\sigma^\sigma(\mathbf{r}_2)} \right). \quad (10)$$

where

$$\rho_{\text{cond}}^{\sigma,\sigma}(\mathbf{r}_2 \mid \mathbf{r}_1) = \frac{\gamma_{\text{cond}}^{\sigma,\sigma}(\mathbf{r}_2 \mid \mathbf{r}_1)}{N^\sigma - 1}, \quad (11)$$

which guarantees the normalisation of $\gamma_{\text{cond}}^{\sigma,\sigma}$ to 1, and

$$\sigma^\sigma(\mathbf{r}) = \frac{\rho^\sigma(\mathbf{r})}{N^\sigma}, \quad (12)$$

is the marginal probability, also known as the shape function [64–66].

Thus, in the present context, $D_{\text{KL},\text{XC}}$ is interpreted as the amount of information gained when the the PDF $\rho_{\text{cond}}^{\sigma,\sigma}$ is used to describe the electronic system, instead of σ^σ . Therefore, from Equations (8), (10) and (11) one can conclude that $D_{\text{KL},\text{XC}}$ provides a measurement of the information content of the exchange-correlation hole density, $\rho_{\text{XC}}^\sigma(\mathbf{r}_2 \mid \mathbf{r}_1)$. This interpretation apparently differs from that employed previously [25]. There, $D_{\text{KL},\text{XC}}$ is employed to reveal the localisation of electrons in space, in such a way that small values of $D_{\text{KL},\text{XC}}$ are associated with regions in which, the conditional probability is close to the marginal distribution; which indicates that electrons are not strongly correlated and; hence, are delocalised. On the other hand, high values of $D_{\text{KL},\text{XC}}$ correspond to regions in which the influence of the reference electron is large, that is, to regions where the electron pair is highly correlated, which is associated with electron localisation. Thus, this interpretation just recasts the manner under which $D_{\text{KL},\text{XC}}$ measures the reciprocal electron correlation, via the *same-spin* Fermi and Coulomb holes. After taking into account the approximated scaling of $D_{\text{KL},\text{XC}}$ with the number of σ -spin electrons, a general descriptor of electron localisation in the space was introduced:

$$\chi_{\text{XC}}(\mathbf{r}_1) = (N^\alpha - 1) D_{\text{KL},\text{XC}}(\mathbf{r}_1) f_{\text{cut}}(\mathbf{r}_1), \quad (13)$$

where f_{cut} is a cut-off function that goes smoothly to zero for negligible density values ($\rho_{\text{cut}} = 1.0 \times 10^{-4}$ a.u.),

$$f_{\text{cut}}(\mathbf{r}) = \frac{1}{2} \left(1.0 + \text{ERF} \left[0.5 \log_{10} \left(\frac{\rho(\mathbf{r})}{\rho_{\text{cut}}} \right) \right] \right). \quad (14)$$

Here, ERF is the error function defined in such a way that $f_{\text{cut}} = 0.5$ at distances satisfying $\rho(\mathbf{r}) \rightarrow \rho_{\text{cut}}$. Our previous studies on χ_{XC} , using density functional theory (DFT) calculations and assuming a monodeterminantal approximation for the calculation of the pair density, reveal that χ_{XC} depicts the region where electrons are spatially localised with astonishing success and in addition produce a clear differentiation between localisation basins that can be traced to the fluctuation in the average number of electron in these regions. This observation confirms our original hypothesis: ‘electron localisation is encoded in the information content of the pair density’.

2.3. Approximated pair-density expression from the natural orbitals

The calculation of χ_{XC} , Equation (13), involves the access to the *same-spin* pair density at the level of theory of the calculation. For the cases where the monodeterminantal approximation is employed, like Hartree–Fock and DFT, the computation of χ_{XC} is very simple. For correlated wave functions the situation is slightly different (at least from the computational point of view). In principle, it is possible to obtain access to the exact *same-spin* pair density from a linear combination of Slater determinant, for example a CASSCF or CISD wave–function, or eventually, the use of optimised orbital expansion in MP2 or CCSD. However, our experience with the computation of χ_{XC} for the F_2 molecule using a CASSCF wave–functions (or an equivalent GVB one) with a large grid of points and medium basis set was disappointing due to the proliferation of non-negligible term in the pair density expansion and the fact that we need to recalculate the pair density at each point of the grid. For this reason, we look for an alternative and approximated approach able to circumvent this technical issue. The central idea is to obtain the pair density, as defined in Equation (1); without resorting to a correlated wave–function expansion but using its natural orbital expansion and the associated occupation numbers which are easily accessible in most of the modern electronic structure programs.

Here, it is assumed that the reduced first-order matrix can be expressed as a combination of n_{NO} orthogonal Natural Orbitals (NOs), $\{\chi_i^\sigma\}$,

$$\gamma^\sigma(\mathbf{r}, \mathbf{r}') = \sum_{i=1}^{n_{\text{NO}}} \eta_i^\sigma \chi_i^\sigma(\mathbf{r}) \chi_i^\sigma(\mathbf{r}'). \quad (15)$$

The η_i^σ are the occupation numbers for σ spin natural orbitals, which fulfill the sum rule,

$$\sum_i \eta_i^\sigma = N^\sigma. \quad (16)$$

The diagonal of $\gamma(\mathbf{r}, \mathbf{r}')$ is the electron density, meaning that $\rho^\sigma(\mathbf{r}) = \gamma^\sigma(\mathbf{r}, \mathbf{r})$. For a Hartree–Fock wave–function, the pair density can be written exactly from the reduced first-order matrix as in the following:

$$\Gamma_{\text{HF}}^{\sigma\sigma}(\mathbf{r}_1, \mathbf{r}_2) = \frac{1}{2} \left(\rho_{\text{HF}}^\sigma(\mathbf{r}_1) \rho_{\text{HF}}^\sigma(\mathbf{r}_2) - |\gamma_{\text{HF}}^\sigma(\mathbf{r}_1, \mathbf{r}_2)|^2 \right). \quad (17)$$

It is important to note that the previous equation coincides with the definition in Equation (6). It is possible to define a zero-order pair density for an explicit correlated level using the same expression of Equation (17); however, the correlated $\gamma^\sigma(\mathbf{r}, \mathbf{r}')$ has to be employed:

$$\Gamma_X^{\sigma\sigma}(\mathbf{r}_1, \mathbf{r}_2) = \frac{1}{2} \left(\rho^\sigma(\mathbf{r}_1) \rho^\sigma(\mathbf{r}_2) - |\gamma^\sigma(\mathbf{r}_1, \mathbf{r}_2)|^2 \right). \quad (18)$$

The previous equation obviously satisfies the antisymmetry requirement of the true pair density, Equation (3). Unfortunately, it violates the sum rule of Equation(4), because any exchange term, similar to the one derived in the Hartree–Fock method, integrates solely to the number of electrons for a single Slater determinant. For this reason an additional term to Equation (18) has to be included as follows:

$$\begin{aligned} \Gamma_{XC}^{\sigma\sigma}(\mathbf{r}_1, \mathbf{r}_2) &= \Gamma_X^{\sigma\sigma}(\mathbf{r}_1, \mathbf{r}_2) + \frac{1}{2} \Gamma_C^{\sigma\sigma}(\mathbf{r}_1, \mathbf{r}_2) \\ &= \frac{1}{2} \left(\rho^\sigma(\mathbf{r}_1) \rho^\sigma(\mathbf{r}_2) - |\gamma^\sigma(\mathbf{r}_1, \mathbf{r}_2)|^2 \right) \\ &\quad + \Gamma_C^{\sigma\sigma}(\mathbf{r}_1, \mathbf{r}_2). \end{aligned} \quad (19)$$

The three contributions appearing in Equation (19) can be interpreted as the uncorrelated Coulomb part, the Hartree–Fock-like exchange interaction, and the correlation correction, respectively. In this particular partition, the large part of the pair density is dominated by the Coulomb and the Hartree–Fock like exchange terms that depend on the natural orbital expansion, while the only unknown term is the relatively small $\Gamma_C^{\sigma\sigma}(\mathbf{r}_1, \mathbf{r}_2)$ component. This partition of $\Gamma_{XC}^{\sigma\sigma}(\mathbf{r}_1, \mathbf{r}_2)$ was suggested for first time by Levy in 1987 [67], however, it appears naturally in the cumulant expansion of the density matrix [68]. Some characteristics of $\Gamma_{XC}^{\sigma\sigma}$, including scaling, bounds, convexity, and asymptotic behaviour are discussed by Levy [67]. Approximated expressions for $\Gamma_C^{\sigma\sigma}(\mathbf{r}_1, \mathbf{r}_2)$ in terms of the natural orbital expansion have been proposed in the literature in the frame of the Density Matrix Functional Theory. An historical account of this problem is presented by Piris [69, 70]. At this point, it is important to point out that the pair density must satisfy certain conditions to ensure the reliability of its derivation from an antisymmetric N-electron wave–function. These requirements are known

as the N-representability conditions. The sets of conditions that guarantee N-representability of the second-order density matrix [71–74] as well as the conditions associated to the pair density are known [75] (the latter ones are implicit in the seminal work of Garrod and Percus [72]). Some approximated conditions for the pair density have been also proposed [70, 76–83]. The implementation in practical applications of some (not necessarily all) N-representability conditions has evolved with great success in the last decade. As a result, the N-representability problem became the basic ingredient of the Density Matrix Functional Theory [69, 70, 83–85]. The first approximate relation for the reduced second-order matrix was proposed by Müller in 1984 [86], while the first natural orbital functional for the second-order density matrix was proposed by Goedecker and Umrigar in 1998 [87]. Then, Buijse and Baerends proposed a functional that removes some restrictions of the Goedecker and Umrigar [88], and Holas generalised the Goedecker and Umrigar functional which preserve the sum rules [89]. Recently, Piris has proposed a correction based on a cumulant expansion that systematically enforces many of the N-representability conditions of the pair density [85]. However, to our knowledge a suitable expression of the pair density in terms of the natural orbital expansion that fulfills all the N-representability conditions has not yet been found. We need to mention at this point that a comparison of different approximations to the pair density in the context of the ELF have been reported by Feixas *et al.* [90], and a condition for the intracule of the pair density that is relevant for the study of non-covalent interactions have been found by Via-Nadal *et al.* [91]. In the present work, we follow a more pragmatic strategy taking advantage of the fact that the natural orbital expansions can be obtained in advance by means of standard procedures. Thus, the pair density is constructed by exploiting some restricted set of conditions, Equations(2)–(6).

In order to obtain an expression to $\Gamma_C^{\sigma\sigma}(\mathbf{r}_1, \mathbf{r}_2)$, the following approximated exchange-like *ansatz* is considered:

$$\Gamma_C^{\sigma\sigma}(\mathbf{r}_1, \mathbf{r}_2) = \sum_{i=1}^{n_{\text{NO}}} \sum_{j=1}^{n_{\text{NO}}} [\alpha_{ij} \chi_i^\sigma(\mathbf{r}_1) \chi_i^\sigma(\mathbf{r}_1) \chi_j^\sigma(\mathbf{r}_2) \chi_j^\sigma(\mathbf{r}_2) - \beta_{ij} \chi_i^\sigma(\mathbf{r}_1) \chi_j^\sigma(\mathbf{r}_1) \chi_j^\sigma(\mathbf{r}_2) \chi_i^\sigma(\mathbf{r}_2)]. \quad (20)$$

The parameters $\{\alpha_{ij}\}$ and $\{\beta_{ij}\}$ are introduced to fulfill as close as possible the conditions of Equation(2)–(5). For instance, it is easy to show that the antisymmetry requirement, Equation(3), implies the following constraint:

$$\alpha_{ij} = \beta_{ij}, \quad (21)$$

whereas the requirements of Equations (4) and (5) hold by observing that each natural orbital occupation

number, η_i^σ , has to obey the following sum rule:

$$\sum_{j \neq i} \alpha_{ij} = \eta_i^\sigma (\eta_i^\sigma - 1). \quad (22)$$

Finally, the conditions of Equations(22) and (23) guarantee the requirement of Equation (6). However, with the purpose of further simplifying the introduction of the previously-commented constraints, the $\{\alpha_{ij}\}$ and $\{\beta_{ij}\}$ parameters are approximated as follows:

$$\alpha_{ij} = \beta_{ij} = -a_i a_j. \quad (23)$$

In this way, only one set of unknown parameters $\{a_i\}$ for each natural orbital has to be determined, and the easiest manner of finding these parameters is through the minimisation of the χ^2 functional.

$$\chi^2 = \sum_i^{n_{\text{NO}}} \left(\eta_i^\sigma (\eta_i^\sigma - 1) + \sum_{j \neq i} a_i a_j \right)^2. \quad (24)$$

With the set of parameters $\{a_i\}$ determined, χ_{XC} Equation (13), from correlated wave-functions can be readily computed.

2.4. The information content of the coulomb hole

In order to obtain a more detailed description of electronic systems that includes the effects of electron correlation, we have computed the Kullback–Leibler divergence between the conditional pair density obtained at some correlated level, $\gamma_{\text{cond,corr}}^{\sigma,\sigma}(\mathbf{r}_2 | \mathbf{r}_1)$, and its Hartree–Fock counterpart, $\gamma_{\text{cond,HF}}^{\sigma,\sigma}(\mathbf{r}_2 | \mathbf{r}_1)$:

$$D_{\text{KL,C}}(\mathbf{r}_1) = \frac{1}{N^\sigma - 1} \int d\mathbf{r}_2 \gamma_{\text{cond,corr}}^{\sigma,\sigma}(\mathbf{r}_2 | \mathbf{r}_1) \log_2 \times \left(\frac{\gamma_{\text{cond,corr}}^{\sigma,\sigma}(\mathbf{r}_2 | \mathbf{r}_1)}{\gamma_{\text{cond,HF}}^{\sigma,\sigma}(\mathbf{r}_2 | \mathbf{r}_1)} \right). \quad (25)$$

where according to Equation (8),

$$\gamma_{\text{cond,corr}}^{\sigma,\sigma}(\mathbf{r}_2 | \mathbf{r}_1) = \rho_{\text{corr}}^\sigma(\mathbf{r}_2) + \rho_{XC,\text{corr}}^\sigma(\mathbf{r}_2 | \mathbf{r}_1), \quad (26)$$

and,

$$\gamma_{\text{cond,HF}}^{\sigma,\sigma}(\mathbf{r}_2 | \mathbf{r}_1) = \rho_{\text{HF}}^\sigma(\mathbf{r}_2) + \rho_{X,\text{HF}}^\sigma(\mathbf{r}_2 | \mathbf{r}_1). \quad (27)$$

The first factor in Equation (25) account for the normalisation factor of the conditional pair density. Here, $\rho_{\text{corr}}^\sigma(\mathbf{r}_2)$ is the electron density at the correlated level of theory, and $\rho_{\text{HF}}^\sigma(\mathbf{r}_2)$ is the Hartree–Fock one, and $\rho_{XC,\text{cor}}^\sigma(\mathbf{r}_2 | \mathbf{r}_1)$ is the exchange–correlation hole density for the correlated level, and $\rho_{X,\text{HF}}^\sigma(\mathbf{r}_2 | \mathbf{r}_1)$ is the Hartree–Fock exchange hole density.

In this case, $D_{KL,C}(\mathbf{r}_1)$ can be interpreted as the information gained when the correlated conditional pair density, obtained with the reference electron located at \mathbf{r}_1 , is employed instead of the approximated Hartree–Fock pair density, with the reference electron at the same position. Thus, Equation (25) provides a direct measure of the information content corresponding to the *same-spin* electronic Coulomb hole density at \mathbf{r}_1 , free of the exchange effects which dominates the $D_{KL,XC}(\mathbf{r}_1)$ behaviour. This definition departs from the usual representation of the Coulomb hole that depends on the inter-electronic distance. Nevertheless, the Hartree–Fock density, $\rho_{HF}^\sigma(\mathbf{r}_2)$ in Equation (27), may differ significantly from the correlated one, $\rho_{corr}^\sigma(\mathbf{r}_2)$ in Equation (26), as a consequence, for these cases the amount of information obtained through $D_{KL,C}(\mathbf{r}_1)$ is not necessarily only related to the Coulomb hole, which may lead to wrong conclusions. In spite of the fact that for most systems, the differences between these two electron densities are not significant, it is important to avoid the possibility of spurious results arising for those few cases; therefore, instead of employing conditional pair densities, the hole densities of Equation (8) will be directly used, and with it, $D_{KL,C}(\mathbf{r}_1)$ becomes:

$$D_{KL,C}(\mathbf{r}_1) = - \int d\mathbf{r}_2 \rho_{XC,corr}^\sigma(\mathbf{r}_2 | \mathbf{r}_1) \log_2 \left(\frac{\rho_{XC,corr}^\sigma(\mathbf{r}_2 | \mathbf{r}_1)}{\rho_{X,HF}^\sigma(\mathbf{r}_2 | \mathbf{r}_1)} \right) \quad (28)$$

in this expression, the negative sign is a consequence of the fact that ρ_{XC}^σ is negative everywhere.

Let us emphasise that, as mentioned above, for most systems, the definitions in Equations (25) and (28) are equivalent; however, the discussion that follows will be based on the latter. Since $D_{KL,C}$ is non-negative, it has a well defined lower bound; nonetheless, its upper bound is not clearly defined. An approximated upper limit can be obtained by introducing the inequality $\log_2(x) \leq x - 1$ in Equation (28) and considering the partition $\rho_{XC,corr}^\sigma(\mathbf{r}_2 | \mathbf{r}_1) = \rho_{X,HF}^\sigma(\mathbf{r}_2 | \mathbf{r}_1) + \rho_C^\sigma(\mathbf{r}_2 | \mathbf{r}_1)$. Moreover, since it is known that the exchange effects dominate the exchange-correlation hole; the contribution of $\rho_C^\sigma(\mathbf{r}_2 | \mathbf{r}_1)$ can be considered negligible in comparison to $\rho_{X,HF}^\sigma(\mathbf{r}_2 | \mathbf{r}_1)$; and hence, the first term $\rho_{XC,corr}^\sigma(\mathbf{r}_2 | \mathbf{r}_1)$ in the integrand, can be approximated by $\rho_{X,HF}^\sigma(\mathbf{r}_2 | \mathbf{r}_1)$. After these considerations, the following expression is obtained:

$$D_{KL,C}(\mathbf{r}_1) \leq \int d\mathbf{r}_2 \rho_C^\sigma(\mathbf{r}_2 | \mathbf{r}_1). \quad (29)$$

Following a similar procedure for Equation (25) an expression, in terms of $\rho_{cond,C}^{\sigma,\sigma}(\mathbf{r}_2 | \mathbf{r}_1)$, is obtained,

$$D_{KL,C}(\mathbf{r}_1) \leq \frac{1}{N^\sigma - 1} \int d\mathbf{r}_2 \rho_{cond,C}^{\sigma,\sigma}(\mathbf{r}_2 | \mathbf{r}_1), \quad (30)$$

in other words, the Coulomb hole information content at \mathbf{r}_1 is always lower than the average value of the difference between the hole density and the Hartree–Fock hole density, or alternatively, of the difference between the full conditional probability density and the Hartree–Fock probability pair density.

A simple quantification of the bounds presented in Equations (29) and (30) can be obtained by evaluating the deviation of the correlated wave–function from a single Slater determinantal one. In the particular case where Equation (15) is employed, this deviation depends on how much η deviates from 1 (full occupied) or 0 (unoccupied). Thus, for this wave–function, the inequalities in Equation (29) can be rewritten as:

$$D_{KL,C}(\mathbf{r}_1) \leq \sum_i^{n_{NO}} (\eta_i - \eta_i^2) \equiv \mathcal{N}_C. \quad (31)$$

By taking this result into account, the function measuring the localisation due to the *same-spin* electron Coulomb hole χ_C is defined as:

$$\chi_C(\mathbf{r}_1) = \frac{D_{KL,C}(\mathbf{r}_1)}{\mathcal{N}_C} f_{cut}(\mathbf{r}_1). \quad (32)$$

In the previous equation we use the same cut-off function employed for χ_{XC} , Equation (14).

3. Computational details

The most time–consuming step of the present methodology is the evaluation of the D_{KL} integral of Equation (10) or Equations (25)–(28) for the computation of χ_{XC} and χ_C , respectively. This section describes our effort to implement an efficient computational code for the numerical calculation of the D_{KL} integrals in a grid of points. In all examples presented, the D_{KL} integration was performed numerically by using the Becke’s algorithm, which is particularly suitable in atomic and molecular problems where the integrand is dominated by nuclei basins [92, 93]. In the Becke’s algorithm, the kernel of the Kulback–Leibler divergence, Equation (9), $p(x) \log_2(p(x)/q(x))$, is first decomposed as a combination of functions for each nuclei employing a continuous generalisation of the Voronoi polyhedral scheme [92]. Each nuclear function is then integrated in spherical polar coordinates around each nuclei using a

combination of the Lebedev's quadrature for the angular part [94–96], and the Gauss–Chebyshev quadrature of the second kind for the radial part. We have used Lebedev's quadrature containing 110 integrations points for $D_{\text{KL},XC}$ and 194 integrations points for $D_{\text{KL},C}$. With the present implementation, we obtain six figures of accuracy in the normalisation of the conditional probability density for all levels.

The wave-functions are obtained by using the Gaussian-16 suite of programs [97]. For the noble gas examples and the F_2 molecule the Dunning's aug-cc-pvtz basis set was employed, in the rest of the examples the split-valence 6–31+ G^* basis function was employed. The canonical molecular orbitals, or alternatively the natural orbitals in the case of correlated wave-functions, were extracted from a WFN Gaussian file. The pair density at correlated wavefunctions was calculated from the natural orbital expansion using the approximated approach described in Section 2.3. The approach involves the minimisation of the χ^2 functional of Equation (24), that depends on the natural orbitals occupations numbers and the parameters $\{a_i\}$. This functional was minimised by the Levenberg–Marquardt algorithm [98, 99]. The Levenberg–Marquardt is ideal for minimisation of nonlinear χ^2 type functionals because it interpolates between the Gauss–Newton algorithm and the steepest decent algorithm. Many variations of the Levenberg–Marquardt have been published (see for instance *Numerical Recipes in FORTRAN 90*) [100]. In the present implementation convergence is achieved when the following two criteria are satisfied: (i) convergence in the gradient of χ^2 lower than 1×10^{-3} , (ii) convergence in χ^2 , lower than 1×10^{-7} . With these convergence criteria, the sum rule of Equation (3) for the pair density is satisfied with five figures. The initial value for every coefficient a_i was considered to be the natural orbital occupation number of the i -th orbital, except for *core* orbitals that have an occupation of 1, in which case $a_{\text{core}} = 0$. In few cases, occupation numbers reach unphysical values (could be larger than 1 or lower than 0), these cases can occur either by a lack in the N -representability conditions (for example at the MP2 level) or due to small numerical errors in very large systems. In the actual implementation of the code, we enforce the occupation numbers to be between 0 and 1; that is, if the occupation number is larger than 1 the occupation is set to 1, and if it is negative is set to 0. For our test cases, this problem produces – in the worse case – an error near 0.05% in the sum rule of Equation (16).

In order to use in an efficient way our computational resources an hybrid parallelisation that use both MPI (Message Passing Interface) and OpenMP (Open Multi-Processing) are employed. The combination of

a coarse-grained parallelisation of the Becke algorithm with MPI and an underlying fine-grained parallelisation of individual MPI-tasks for a grid of points allows to use the maximum number of processors efficiently. The sending and receiving messages is achieved through standards libraries calls, so the present program is portable to any architectures for which MPI Libraries are available. The last version of the FORTRAN 90/MPI/Open-MP code to create the grids of points, along with technical documentation and test cases, is available from the authors under request.

4. Results and discussion

With the purpose of assessing the performance of χ_{XC} , obtained from correlated methods, and its associated χ_C to visualise the *same-spin* component of the Coulomb hole, we present in this section calculations for the Ne and Ar noble gases, the F_2 molecule which is expected to be highly affected by electron correlation, and some none-covalent systems.

4.1. Noble gases

χ_{XC} calculated at the RHF level has been previously demonstrated that is a good tool to obtain the shell structure of atoms in the sense that it reproduces the expectation of the number of electrons per shell with a deviation of 0.05–0.15 [25]. In order to check the effect of the electronic correlation on χ_{XC} and χ_C for the ground state of Ne and Ar atoms, we perform calculations at the CISD/aug-cc-pvtz level of theory. Figure 1 shows the results for χ_{XC} at the RHF (solid line) and CISD (dotted line) levels of theory, and for χ_C at the CISD level (dashed line).

In the two cases we observe the following trends: (i) the observed tendencies in χ_{XC} are similar to the observed using ELF [12, 101–103] or the one electron potential [14]; (ii) the minima and maxima of χ_{XC} are located at the same distance of the nuclei regardless the level of theory, that means that the radius and occupation of the each shell is almost independent on the level of theory; (iii) the value of χ_{XC} is almost identical for inner shells; however a small decrease between 2.2% and 2.5% is observed in the valence shell using CISD when compared to RHF, that means that the electron correlation tends to decrease the localisation of valence electrons due to the unoccupation of the RHF orbitals and the occupation of the virtual ones; (iv) the plot of χ_C (dotted curve) is almost constant from the origin to the border between the inner and the valence shells; furthermore, it presents a minimum in the region of the valence shell and local maxima in the region where χ_{XC} changes

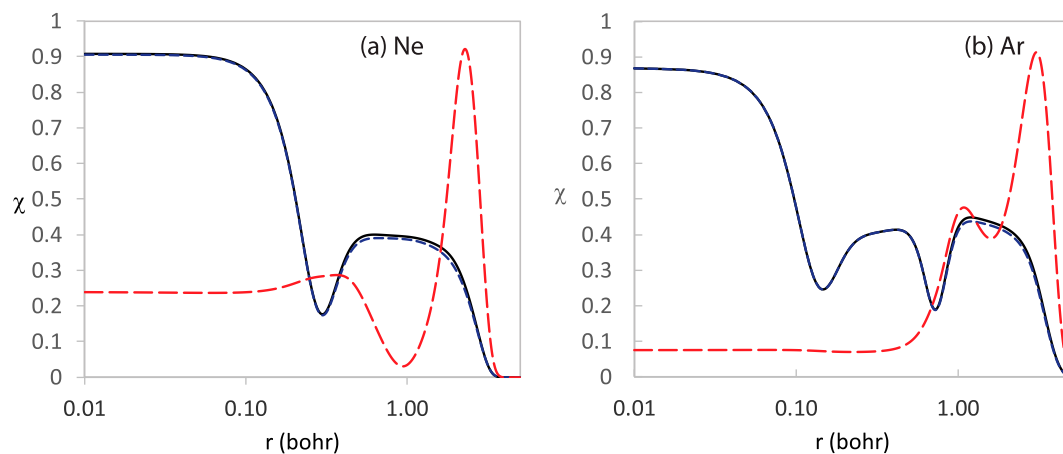


Figure 1. Plots of χ_{XC} at the RHF (solid line) and CISD (dotted line) and χ_C for CISD (dashed line) as a function of the distance to the nuclei for the case of noble gas atoms: (a) Ne and (b) Ar.

drastically. In view of the latter, it can be suggested that the maxima information attained by the correlation hole is located when the reference electron is placed at the atomic borders.

4.2. The F_2 molecule

In this section, the behaviour of χ_{XC} and χ_C is analysed at two interatomic distances for the F_2 molecule, whose properties are expected to be significantly affected

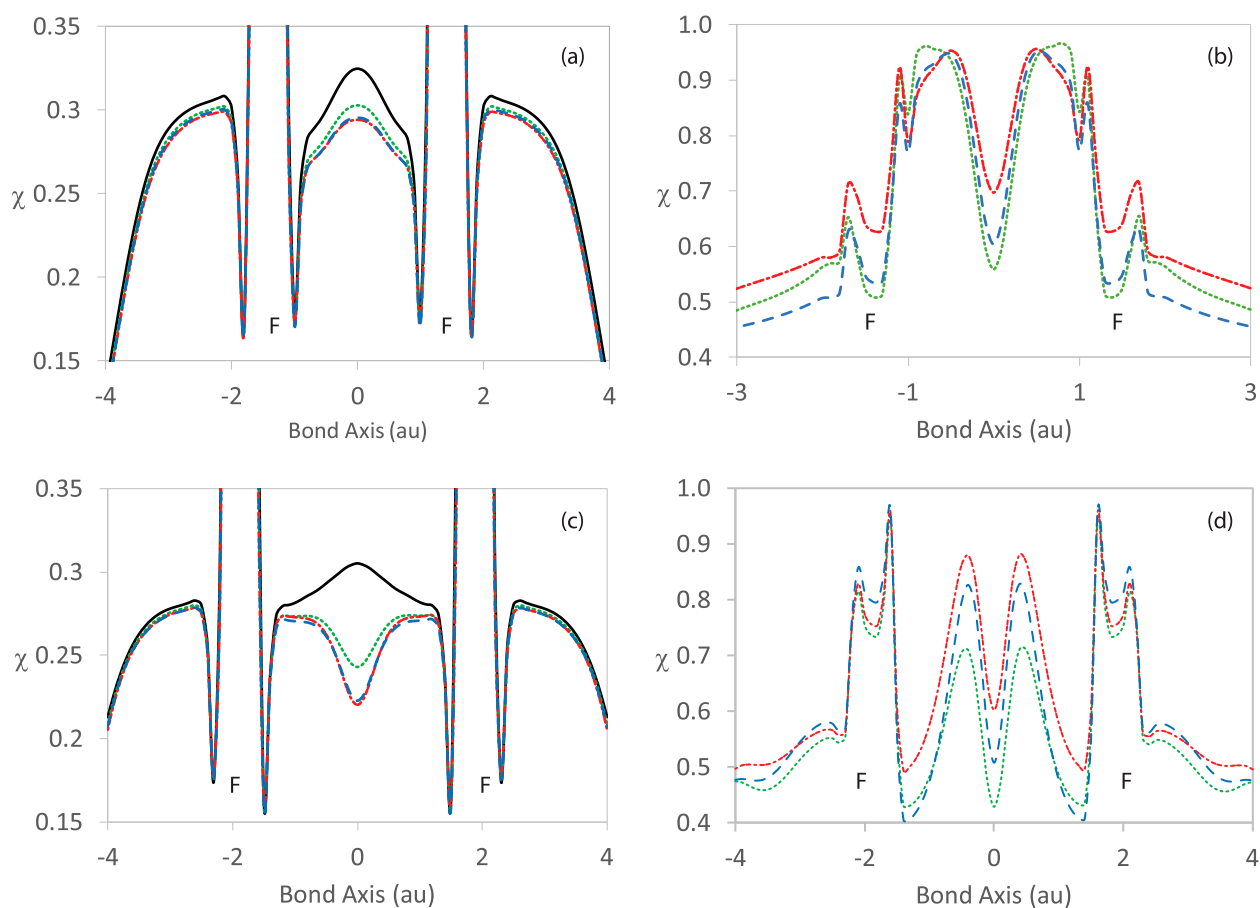


Figure 2. Plots of χ_{XC} and χ_C along the bond axis (in atomic units) of the F_2 molecule. (a) χ_{XC} and (b) χ_C at $R(F-F) = 1.4 \text{ \AA}$; (c) χ_{XC} and (d) χ_C at $R(F-F) = 2.0 \text{ \AA}$. Levels of theory: RHF (solid), CISD (dotted), MP2 (dashed) and CCSD (double dashed).

by the inclusion of electron correlation. It is important to remind that the Hartree–Fock approximation was shown to be inappropriate for describing the F_2 molecule since this method produces negative binding energy values [104–112], suggesting that the stability of the F–F bond is totally due to the effects of the electron correlation. Figure 2(a ,c) shows plot of χ_{XC} along the bond axis at $R(F-F) = 1.40 \text{ \AA}$ and $R(F-F) = 2.00 \text{ \AA}$, respectively, for four different levels of theory, namely: RHF (solid), CISD (dotted), MP2 (dashed) and CCSD (double dashed). The basis set in all cases was the Dunning's aug-cc-pvtz. Figure 2(b ,d) shows the same plots for χ_C .

At a $R(F-F)$ distance of 1.40 \AA (near the equilibrium distance, Figure 2(a)), the topology of χ_{XC} along the bond axis is the same for all levels of theory: two large basins containing the core electrons with a population of about 2.30–2.40 electrons and a small basin at the centre of the bond with a population that decrease from 0.42 electrons for RHF to 0.22 electrons for CCSD are observed. Figure 2(a) also shows that the χ_{XC} maximum value obtained at the correlated levels decreases at the central basin with respect to the RHF result, and with it its electronic occupation number varies from 0.325 at RHF, 0.307 for CISD, 0.301 for MP2 and 0.299 for CCSD. Therefore, the drain of the Hartree–Fock orbitals in favour of the virtual ones tends to remove electron density from the central basin and reduce the degree of localisation. The central maxima reduction, due to the occupation of the virtual orbitals, can explain the unconventional positive value of the Laplacian of the electron charge density, $\nabla^2\rho(r)$, at the F_2 bond critical point [113], which indicates an electronic density migration from the bonding region to other molecular zones. The latter supports the idea of the charge-shifting character of the F–F bond, whose stability requires the resonance between

covalent and ionic structures as well as the dynamical correlation [114]. At a distance $R(F-F)$ distance of 2.00 \AA , Figure 2(c), the central basin splits in two symmetric basins for the correlated methods, whereas for the RHF level, it remains unimodal. It is important to point out that this splitting is also observed using the ELF at the equilibrium distance [103]. The χ_C function (Figure 2(b ,d)) exhibits six maxima, symmetrically distributed about the bond centre. In the two figures, the absolute maxima are approximately at the border region separating the F core electron basins (corresponding to the largest χ_{XC} maxima on the F nuclei) and the bonding basin (associated with the central χ_{XC} maximum of Figure 2(a) or the two small central maxima in Figure 2(c)). Two maxima are observed at each side of the central basin χ_{XC} maximum in Figure 2(a) or the central minima of Figure 2(c). On the other hand, a minimum χ_C value is at the bond centre, two relative minima are at the centre of the F core electron basins and two more relative minima are located on each F at the core basin edges. From this set of results, and by comparing $\chi_{XC}(\mathbf{r}_1)$ and $\chi_C(\mathbf{r}_1)$, it is possible to conclude that due to the Coulombic interaction, $\chi_C(\mathbf{r}_1)$ has its minima at or around the positions where $\chi_{XC}(\mathbf{r}_1)$ has its maxima, which corresponds to zones of electronic localisation. Also, as a consequence of this correlation effect, the $\chi_C(\mathbf{r}_1)$ information content is maximum at some distance from the electronic population maxima, coinciding with the zones where $\chi_{XC}(\mathbf{r}_1)$ changes rapidly or reaches a minimum, at the border between shells: the inter-shell region between core and valence electrons, and between core and lone-pair electrons. In other words, these results indicate that the Coulomb hole is greater near the regions where $\chi_{XC}(\mathbf{r}_1)$ shows a maximum: near the molecular centre and around the core electron basins.

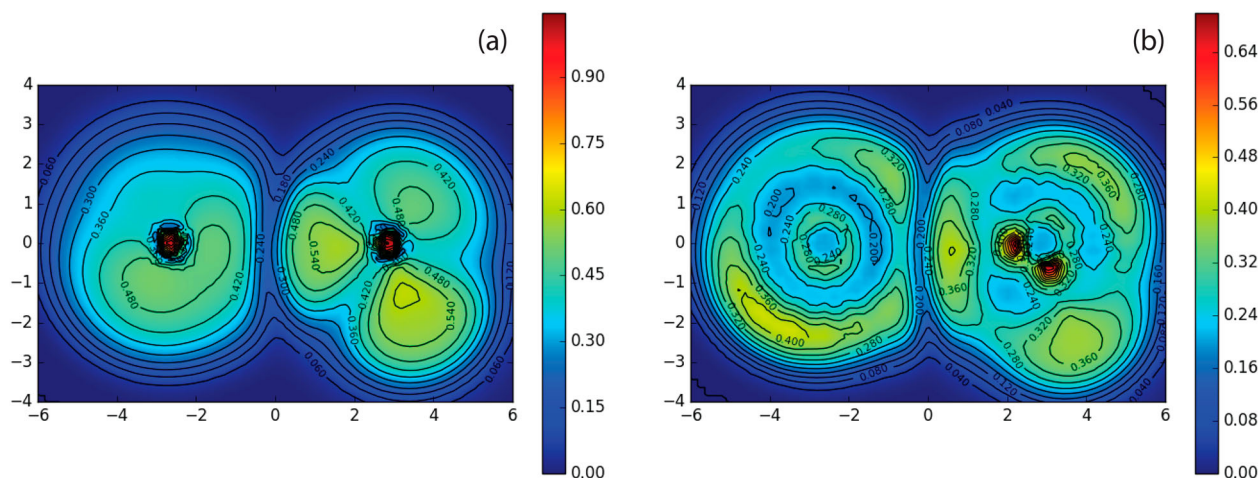


Figure 3. (a) χ_{XC} and (b) χ_C for the water dimer.

4.3. Non-covalent interactions from the information content of the Coulomb hole

In this section, a number of non-covalent bonded systems, namely, the water and the *T*-shaped benzene dimers, and different HF_{*n*} (*n* = 1, 2, 3, 4, 5, and 6) clusters are discussed. Here, the χ_C and χ_{XC} results are presented graphically to facilitate the discussion of the role of electron correlation in these system formation. The calculations were performed at the MP2/6-31+G* level, adopting the geometries reported in the S22 benchmark data set [115, 116].

For the water dimer, Figure 3(a, b) exhibit, respectively, the χ_{XC} and χ_C functions contour maps on the hydrogen bond molecular plane. The analysis of the results in Figures 3(a) leads to conclude that the topology and behaviour of χ_{XC} are close to those reported for this system described by ELF [12, 117–124]. Therefore, in order to gain further insights on this system formation, the discussion will be focused on the χ_C function. From Figure 3(b), one observes that χ_C shows maxima in the inter-shell region between the oxygen core electron basin and the covalent O–H bond basin, where, as shown in Figure 3(a), χ_{XC} , i.e. the electronic occupation, has a minimum. In other words, this result shows that the correlation between *same-spin* electron tends to reduce the electron–electron repulsion by maximising the Coulomb holes around the regions where the electronic occupation, i.e. χ_{XC} , is a maximum. This result is, qualitatively similar to that obtained for the F₂ molecule, and a similar behaviour is observed around the region where the hydrogen bond interaction takes place. Thus, it is observed that a χ_C maximum is located in the region where χ_{XC} reaches a local minimum. This behaviour is further evidenced by the changes in the χ_C value in the outer region of the hydrogen atom, from 0.36 for the free water molecule, to 0.42, for the hydrogen atom involved in the water dimer hydrogen bond. As it will be seen from the following examples, this behaviour can be considered as a signature of the hydrogen bond existence.

Next, the HF_{*n*} (*n* = 1, 2, 3, 4, 5, and 6) clusters are considered. These systems have been chosen, because they are among the clusters with the largest detectable gas phase cooperative effects [27]. Additionally, with the exception of the dimer, all these clusters have highly-symmetric planar cyclic geometries; fact that simplifies considerably the analysis [27, 28, 125]. Before continuing, it is important to mention that simple electrostatic models, or pair-wise additive potential models, predict that the binding energy per hydrogen bond (BEHB) remains approximately constant with the variation in the number of cluster members, i.e. the hydrogen bond strength remains approximately the same, regardless of the cluster

size. Nevertheless, as it has been extensively discussed, this is not the case. Thus, for instance, one of the major finding of Ref. [27] is that in the HF_{*n*} clusters, the cooperative effects are the main cause for the formation of stable hydrogen-bond networks. A conclusion that was corroborated after performing a detailed analysis of the topology of the ELF [125]. Moreover, this conclusion was further supported by a many body energy decomposition analysis, which revealed that the three and four body terms, besides being non-negligible, must be included in the system description, if a correct qualitative behaviour is to be obtained [28]. As a consequence of these results, the electron correlation effects are expected to be of great importance, and these effects become more significant for the system stabilisation, as the cluster size increases.

In Figure 4, the χ_C results for the considered HF_{*n*} clusters are displayed as contour maps on the cluster planes. As obtained for the water dimer, two maxima are observed for each monomer, one located in the inter-shell region, between the fluor core electron basin and the covalent F–H bond basin, and the second one around the hydrogen bond region, near the hydrogen atom. Inspection of Figure 4 shows that for the dimer, the behaviour resembles the properties of the water dimer. Nevertheless, for the other clusters it is clear that the value of the second maximum increases with the cluster size, becoming comparable with that of the maximum located around the inter-shell region. Even more interestingly, it is observed that for the larger clusters, the χ_C values become approximately constant throughout the whole molecular network. Recalling that the *same-spin* correlation tends to maximise the Coulomb hole, around the regions where the electronic occupation is maximum, the obtained χ_C value homogeneity leads to think that the electronic occupation is also approximately uniform throughout the whole system. This allow us to state that the larger the cluster size the more homogeneously distributed the electrons are over the whole hydrogen bonding network. It was previously concluded [27, 125], that this increase in the electronic density delocalisation around the whole cluster is correlated with the BEHB. Further evidence for this conclusion can be drawn from the plot at the bottom-right of Figure 4. The results there show that BEHB correlates well with the value of the χ_C maxima around the hydrogen bond region, close to the hydrogen atom (i.e. $R^2 = 0.9995$ for a quadratic fitting). This quadratic correlation form is indicative of the rapid growth in the cluster stabilisation as the electron correlation increases, result that evidences the connection between the correlation and the cooperative effects, characteristic of the hydrogen bonded clusters.

It is well-known that the benzene dimer stabilisation is almost exclusively due to non-covalent interactions, and its understanding has posed substantial challenges, from both, theoretical and experimental points of view [126–135]. A complete characterisation of the factors determining the formation of the stable geometries of this kind of systems is still lacking. In general, it is assumed that the *same-spin* correlation plays an important role in the formation of dispersion interacting systems [132–135] hence, the Coulomb hole analysis could be valuable to obtain information on the behaviour of these systems. In this direction, Figure 5(a,b), display, respectively, the results for χ_{XC} and χ_C , as contour maps

on the plane of the benzene interacting with the π electronic density of the second benzene. It is found that the χ_{XC} results are similar to those obtained for an isolated benzene molecule; however, close inspection shows a slight difference in the electronic occupation pattern of the C–H bond directly interacting with the π electronic density of the other molecule. There, a small decrease in this bond outer χ_{XC} maximum is obtained, a result that leads to think that a small decrease in the electronic density occurs around the hydrogen atom directly interacting with the second molecule. Again, to get further insights on this behaviour let us examine the χ_C function. These function results indicate that, as expected, the

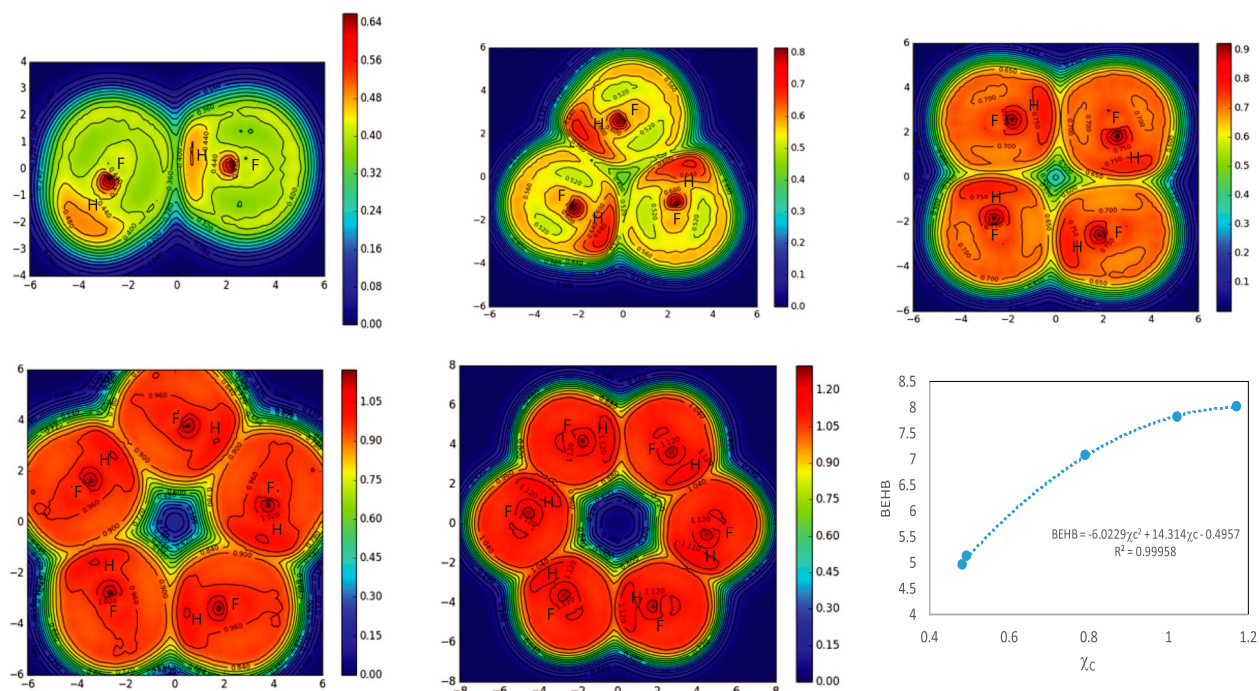


Figure 4. χ_C for the hydrogen fluoride clusters from the dimer to the hexamer. A plot of the Binding Energy per Hydrogen Bond (BEHB in kcal/mol) versus the maxima of χ_C at the Hydrogen border.

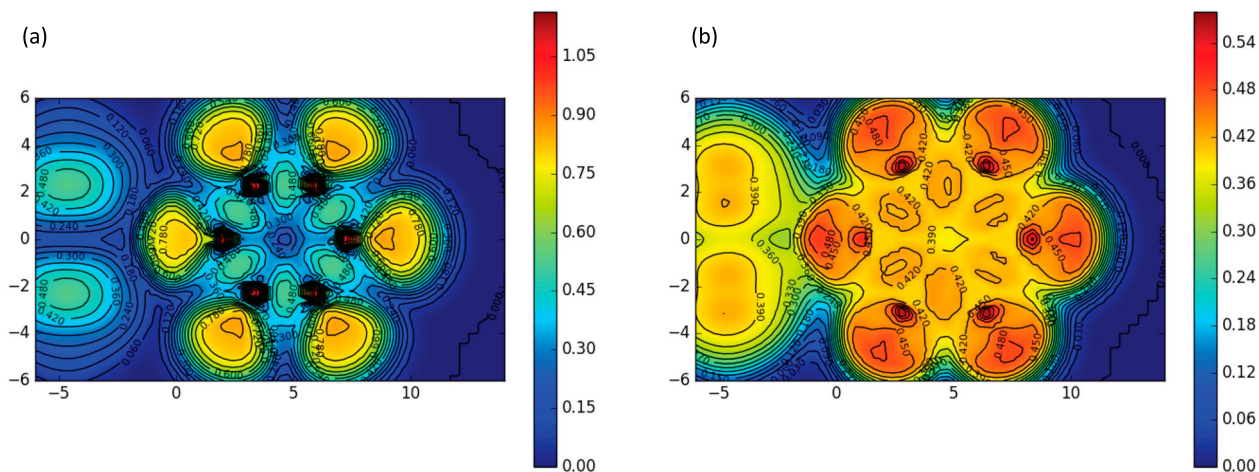


Figure 5. (a) χ_{XC} and (b) χ_C for the benzene dimer *T*-shape.

electronic density is delocalised around the whole molecular basin: the χ_C values about the whole inter-molecular region are non-negligible and approximately constant, behaviour similar to that discussed for the HF_n clusters.

5. Summary and final remarks

In this work, we have used two information-based functions, aimed to describe separately the behaviour of the Fermi and the Coulomb holes, and to visualise the regions in which they are localised in space. The first of these functions, χ_{XC} , provides the amount of electronic system information gained when describing the system by its conditional probability, $\rho_{\text{cond}}^{\sigma,\sigma}$, in comparison to that obtained by describing it by its marginal probability, i.e. electronic density. Hence, this function can be considered a measure of the extension of the Exchange-Correlation hole density in space, providing the electron localisation regions associated to core, bonding and lone pair electrons. It is found that these regions are revealed with the same, and in some cases even better, precision than that obtained from the widely employed ELF [25]. The second function, χ_C , provides the information gained when going from describing the electronic system by the uncorrelated Hartree-Fock pair density (i.e. the only-Exchange hole density) to an correlated one (i.e. the associated Exchange-Correlation hole density). Therefore, χ_C can be considered a measure of the extension of the *same-spin* Coulomb hole density at a reference position; and consequently, it can be used to analyse the effects of the electron correlation in molecular system behaviour. It is also worth emphasising that the characterisation of the electron correlation and their effects provides the basis for understanding non-classical bonds and their behaviour. Here, the χ_{XC} and χ_C functions have been calculated by using correlated wave-functions, and this has been achieved by employing an approximated methodology, that allows the pair density to be computed by using natural orbitals and their occupancy numbers which are accessible from most of the modern electronic structure calculation programs. We have decided to use approximated pair densities to reduce the computational cost that would represent the computation of the exact one from correlated levels of theory. It is important to notice that this approximated method, fulfils some of the symmetry conditions and sum rules (Equations (3)–(5)), required by the exact pair density, and we have checked these conditions as a criteria of confidence in our pair density. We need to admit that more stringent criteria could be used in the future, for example a comparison between the approximated energies (using the computed pair density) and that obtained without approximation. By comparing the $\chi_{XC}(\mathbf{r}_1)$ and

$\chi_C(\mathbf{r}_1)$ results, it has been noticed that, as a result of the Coulombic interactions, the last function has its minima at or around the positions where the first has its maxima, which are located about the electronic localisation regions. Also, as a consequence of this dynamical Coulombic correlation effect, it has been observed that the $\chi_C(\mathbf{r}_1)$ information content is maximum at the border regions between shells, at some distance from the electronic population maxima, coinciding with the regions where $\chi_{XC}(\mathbf{r}_1)$ changes rapidly: the inter-shell region between core and valence electrons, and between core and lone-pair electrons. These results confirm that the Coulomb hole is greater close to the molecular bonding and lone pair basin centres. Thus, for each considered X–H bond, with X = O, F and C, two maxima have been observed, the largest one located in the inter-shell region between the X core electron basin and the covalent X–H bond basin, and the second one around the external region of the hydrogen atom. The characterisation of the $\chi_{XC}(\mathbf{r}_1)$ and $\chi_C(\mathbf{r}_1)$ functions has also allowed a preliminary analysis of non-covalently bonded systems. Here three widely studied systems have been considered; the water and the T-shaped benzene dimers and various HF_n clusters. For the HF_n clusters, the homogeneity of the χ_C value obtained throughout the whole cluster, has led to think that the electronic occupation is also approximately uniform throughout the whole hydrogen bonded system, with the electronic density delocalisation becoming larger with the cluster size. The excellent correlation found between the BEHB and the value of the χ_C maxima around the hydrogen bond region, close to the hydrogen atom, has permitted to confirm previous results relating electronic density delocalisation around the whole cluster with the increase in the cooperative effects. For the T-shaped benzene dimer, the χ_C function inspection has revealed a non-symmetrical pattern, that points out to the existence of a small electronic depletion in the half of the molecule closer to the second benzene. Moreover, analysis of the χ_C behaviour of the C–H bond closer to the second molecule, has showed a deviation of the pattern mentioned above, indicating that the C–H bond electronic density becomes more homogeneously distributed throughout the bond and becomes smaller near the interaction region. These results, have allowed us to conclude that for this weak dispersive intermolecular interaction, the *same-spin* correlation, associated with the intermolecular dispersion interaction, distorts the ring π electronic density, and affects the electronic occupation pattern of the C–H bond directly involved in this non-covalent interaction. These applications point out to the potentiality of χ_{XC} and χ_C in the characterisation of systems formed by non-conventional bonding. There is a link between χ_{XC} and χ_C and electron localisation

function [12, 13], especially its modern formulation based on the analysis of the exchange-correlation hole [14–17, 19–23]. The approach based on non-local exchange correlation model seem particular connected to the information content of the conditional pair density [16, 17, 19].

In spite of the advantages observed for χ_C from the results showed in this work, it is important to introduce some limitations that are important to address in the near future:

- The efficiency in the numerical calculation of the Kullback–Leibler divergency needs to be improve. The performance of the employed parallelised code limits the completeness of the employed basis, the size of the considered systems and the density of the grid points used in the χ_C computation.
- Theoretical efforts to unveil a way to compute DFT pair densities without resorting to mono-determinant approximations have to be carried out in future.
- The present approach should be extended to consider the contribution of different-spin electrons to the Coulomb hole.

The work to overcome these difficulties is in progress, and in subsequents manuscripts, the χ_C calculations will be applied to obtain some deeper insights on problems as charge-shifting bonds, excited states and open-shell systems, where the employment of a correlated level of calculation is mandatory to acquire a better understanding of these system.

Acknowledgements

This work has been performed by employed the resources from the NCU's and USFQ's High Performance Computing systems. L.R, F.J.T. and M.B. highly appreciate the financial support from USFQ's POLIGRANTS 2017–2018.

Disclosure statement

No potential conflict of interest was reported by authors.

References

- [1] S. Shaik, *J. Comput. Chem.* **28**, 51 (2007).
- [2] R.F.W. Bader and M.E. Stephens, *J. Amer. Chem. Soc.* **97**, 7391 (1975).
- [3] R.F.W. Bader, S. Johnson, T.H. Tang, and P.L.A. Popelier, *J. Phys. Chem.* **100**, 15398 (1996).
- [4] R.J. Gillespie, D. Bayles, J. Platts, G.L. Heard, and R.F.W. Bader, *J. Phys. Chem. A* **102**, 3407 (1998).
- [5] X. Fradera, M.A. Austen, and R.F.W. Bader, *J. Phys. Chem. A* **103**, 304 (1999).
- [6] R.F.W. Bader and G.L. Heard, *J. Chem. Phys.* **111**, 8789 (1999).
- [7] R. Ponec and M. Strnad, *Int. J. Quantum Chem.* **50**, 43 (1994).
- [8] D.L. Cooper, R. Ponec, T. Thorsteinsson, and G. Raos, *Int. J. Quantum Chem.* **57**, 501 (1996).
- [9] R. Ponec, *J. Math. Chem.* **21**, 323 (1997).
- [10] R. Ponec, *J. Math. Chem.* **23**, 85 (1998).
- [11] J. Lennard-Jones, *Adv. Sci.* **11**, 136 (1954).
- [12] A.D. Becke and K.E. Edgecombe, *J. Chem. Phys.* **92**, 5397 (1990).
- [13] B. Silvi and A. Savin, *Nature* **371**, 683 (1994).
- [14] M. Kohout, *Int. J. Quantum Chem.* **83**, 324 (2001).
- [15] A. Savin, *J. Mol. Struct. (THEOCHEM)* **727**, 127 (2005).
- [16] P.W. Ayers, *J. Chem. Sci.* **117**, 441 (2005).
- [17] L. Rincon, J.E. Alvarelos, and R. Almeida, *Phys. Chem. Chem. Phys.* **13**, 9498 (2011).
- [18] E. Matito, M. Sola, and M. Duran, *Faraday Discuss.* **135**, 325 (2007).
- [19] J. Angyan, *Int. J. Quantum Chem* **119**, 2340 (2009).
- [20] B. Janesko, G. Scalmani, and M. Frisch, *J. Chem. Phys.* **141**, 144104 (2014).
- [21] B. Janesko, G. Scalmani, and M. Frisch, *J. Chem. Phys.* **12**, 79 (2016).
- [22] B. Janesko, *J. Comp. Chem.* **37**, 1993 (2016).
- [23] B. Janesko, G. Scalmani, and M. Frisch, *Phys. Chem. Chem. Phys.* **17**, 18305 (2015).
- [24] R. Nalewajski, A. Köster, and S. Escalante, *J. Phys. Chem. A* **109**, 10038 (2005).
- [25] A.S. Urbina, F.J. Torres, and L. Rincon, *J. Chem. Phys.* **144**, 244104 (2016).
- [26] L. Rincon, F.J. Torres, and R. Almeida, *Mol. Phys.* **116**, 578 (2018).
- [27] L. Rincon, R. Almeida, D. Garcia-Aldea, and H. Diez y Riega, *J. Chem. Phys.* **114**, 5552 (2001).
- [28] L. Rincon, R. Almeida, and D. Garcia-Aldea, *Int. J. Quantum Chem.* **102**, 443 (2005).
- [29] R. McWeeny, *Rev. Mod. Phys.* **32**, 335 (1960).
- [30] R. McWeeny, *Int. J. Quantum Chem.* **1**, 351 (1967).
- [31] R.J. Boyd and C.A. Coulson, *J. Phys. B* **7**, 1805 (1974).
- [32] E.V. Ludeña, J.M. Ugalde, X. Lopez, J. Fernandez-Rico, and G. Ramirez, *J. Chem. Phys.* **120**, 540 (2004).
- [33] R.A. Fisher, *Math. Proc. Camb. Philos. Soc.* **22**, 700 (1925).
- [34] C.E. Shannon, *Bell Syst. Tech. J.* **27**, 623 (1948).
- [35] R.F. Nalewajski, *Information Theory of Molecular Systems* (Elsevier, Amsterdam, 2006).
- [36] R.F. Nalewajski, *Information Origins of the Chemical Bond* (Nova Science Publishers, New York, 2010).
- [37] R.F. Nalewajski, *Struct. Bonding* **149**, 51 (2012).
- [38] S. Liu, *J. Chem. Phys.* **126**, 191107 (2007).
- [39] C. Rong, T. Lu, and S. Liu, *J. Chem. Phys.* **140**, 024109 (2014).
- [40] S. Liu, C.Y. Rong, Z.M. Wu, and T. Lu, *Acta Phys.-Chim. Sin.* **31**, 2057 (2015).
- [41] S. Liu, *Acta Phys.-Chim. Sin.* **32**, 98 (2016).
- [42] X.Y. Zhou, C. Rong, T. Lu, P. Zhou, and S. Liu, *J. Phys. Chem. A* **120**, 3634 (2016).
- [43] L. Rincon, R. Almeida, P.L. Contreras, and F.J. Torres, *Chem. Phys. Lett.* **635**, 116 (2015).
- [44] Collins and Smith, *Z. Naturforsch A* **48**, 68 (1993).
- [45] J. Ramirez, C. Soriano, R. O. Esquivel, R. P. Sagar, M. Hô, and V. H. Smith Jr, *Phys. Rev. A* **56**, 4477 (1997).

- [46] R. Sagar, R. Ramirez, J.C. Esquivel, M. Ho, and V. Smith, *J. Chem. Phys.* **116**, 9213 (2002).
- [47] A. Nagy and R. Parr, *Int. J. Quantum Chem.* **58**, 323 (1996).
- [48] P. Ziesche, O. Gunnarsson, W. John, and H. Beck, *Phys. Rev. B* **55**, 10270 (1997).
- [49] P. Ziesche, V. H. Smith Jr, M. Hó, S. P. Rudin, P. Gersdorf, and M. Taut, *J. Chem. Phys.* **110**, 6135 (1999).
- [50] P. Ziesche, *J. Mol. Struct. (THEOCHEM)* **527**, 35 (2000).
- [51] N. Guevara, R. Sagar, and R. Esquivel, *Phys. Rev. A* **67**, 012507 (2003).
- [52] A. Grassi, *Int. J. Quantum Chem.* **111**, 2390 (2011).
- [53] C. Matta, M. Sickinga, and P. Ayers, *Chem. Phys. Lett.* **514**, 379 (2011).
- [54] J. Chai, *J. Chem. Phys.* **136**, 145104 (2012).
- [55] D. Alcoba, A. Torre, L. Lain, O. B. Oña, P. Capuzzi, M. Van Raem-donck, P. Bultinck, and D. Van Neck, *Theor. Chem. Acc.* **135**, 153 (2016).
- [56] N. Flores-Gallego, *Chem. Phys. Lett.* **666**, 62 (2016).
- [57] N. Flores-Gallego, *Chem. Phys. Lett.* **692**, 61 (2018).
- [58] C. Amovilli and F. Floris, in *Many-body Approaches at Different Scales*, edited by G. Angilella and C. Amovilli (Springer, Cham, 2018), pp. 187–198.
- [59] S. Kullback and R.A. Leibler, *Ann. Math. Stat.* **22**, 79 (1951).
- [60] S. Kullback, *Statistics and Information Theory* (Wiley, New York, 1959).
- [61] D. MacKay, *Information Theory, Inference and Learning Algorithms* (Cambridge University Press, Cambridge, 2003).
- [62] S.S. Dragomir and V. Gluscevic, *Tamsui Oxford J. Math. Soc.* **17**, 97 (2001).
- [63] A. Sayyareh, *App. Math. Sci.* **5**, 3303 (2011).
- [64] R. Parr and L. Bartolotti, *J. Phys. Chem.* **87**, 2810 (1983).
- [65] P. Ayers, *Proc. Nat. Acad. Sci.* **97**, 1959 (2000).
- [66] F. De Proft, P.W. Ayers, K.D. Sen, and P. Geerlings, *J. Chem. Phys.* **120**, 9969 (2004).
- [67] M. Levy, in *Density Matrices and Density Functional*, edited by J. Erdahl and V. H. Smith (Dordrecht D, Reidel, 1987).
- [68] W. Kutzelnigg and D. Mukherjee, *J. Chem. Phys.* **110**, 2800 (1999).
- [69] M. Piris, *Adv. Chem. Phys.* **134**, 387 (2007).
- [70] M. Piris, *Int. J. Quantum Chem.* **114**, 1169 (2014).
- [71] A.J. Coleman, *Rev. Mod. Phys.* **35**, 668 (1963).
- [72] C. Garrod and J.K. Percus, *J. Math. Phys.* **5**, 1756 (1964).
- [73] D.A. Mazziotti, *Phys. Rev. Lett.* **108**, 263992 (2012).
- [74] D.A. Mazziotti, *Phys. Rev. A* **94**, 032516 (2016).
- [75] P. Ayers, *Phys. Rev. A* **74**, 042502 (2006).
- [76] E.R. Davidson, *Phys. Rev. A*, **1**, 30 (1970).
- [77] P. Ayers and E. Davidson, *Int. J. Quantum Chem.* **106**, 1487 (2006).
- [78] M. Pistol, *Chem. Phys. Lett.* **400**, 548 (2004).
- [79] M. Pistol, *Chem. Phys. Lett.* **417**, 521 (2006).
- [80] M. Pistol, *Chem. Phys. Lett.* **422**, 363 (2006).
- [81] M. Pistol, *Chem. Phys. Lett.* **431**, 216 (2006).
- [82] M. Pistol, *Chem. Phys. Lett.* **449**, 208 (2007).
- [83] M. Rodriguez-Mayorga, E. Ramos-Cordoba, M. Via-Nadal, and E. Matito, *Phys. Chem. Chem. Phys.* **19**, 24029 (2017).
- [84] M. Piris, *Int. J. Quantum Chem.* **106**, 1093 (2006).
- [85] M. Piris, *Int. J. Quantum Chem.* **113**, 620 (2013).
- [86] A.M.K. Müller, *Phys. Lett. A* **105a**, 446 (1984).
- [87] S. Goedecker and C.J. Umrigar, *Phys. Rev. Lett.* **81**, 866 (1998).
- [88] M.A. Buijse and E.J. Baerends, *Mol. Phys.* **100**, 401 (2002).
- [89] A. Holas, *Phys. Rev. A* **59**, 3454 (1999).
- [90] F. Feixas, E. Matito, M. Duran, M. Sola, and B. Silvi, *J. Chem. Theor. Comput.* **6**, 2736 (2010).
- [91] M. Via-Nadal, M. Rodriguez-Mayorga, and E. Matito, *Phys. Rev. A* **96**, 050501(R) (2017).
- [92] A.D. Becke, *J. Chem. Phys.* **88**, 2547 (1988).
- [93] J.M. Perez-Jorda, A.D. Becke, and E. San-Fabian, *J. Chem. Phys.* **100**, 6520 (1994).
- [94] V.I. Lebedev, *USSR Comput. Math. & Math. Phys.* **15**, 44 (1975).
- [95] V.I. Lebedev, *USSR Comput. Math. & Math. Phys.* **16**, 10 (1976).
- [96] V.I. Lebedev, *Siberian Math. J.* **18**, 99 (1977).
- [97] M.J. Frisch, M. J. Frisch, G. W. Trucks, H. B. Schlegel, G. E. Scuseria, M. A. Robb, J. R. Cheeseman, G. Scalmani, V. Barone, G. V. Petersson, H. Nakatsuji, and X. Li, *Gaussian-16 Revision a.03* (Gaussian Inc., Wallingford, CT, 2016).
- [98] K. Levenberg, *Q. Appl. Math.* **2**, 164 (1944).
- [99] D.W. Marquardt, *J. Soc. Ind. Appl. Math.* **11**, 431 (1963).
- [100] W.H. Press, S.A. Teukolsky, W.T. Vetterling, and B.P. Flannery, *Numerical Recipes in Fortran 90, Vol. 2*. (Cambridge University Press, Cambridge, 1996).
- [101] M. Kohout and A. Savin, *Int. J. Quantum Chem.* **60**, 875 (1996).
- [102] M. Kohout and A. Savin, *J. Comput. Chem.* **18**, 1431 (1997).
- [103] E. Matito, B. Silvi, M. Duran, and M. Sola, *J. Chem. Phys.* **125**, 024301 (2006).
- [104] K. Hijikata, *J. Chem. Phys.* **34**, 221 (1961).
- [105] G. Chambaud, B. Levy, and P. Millie, *Theor. Chim. Acta* **48**, 103 (1978).
- [106] A. Bruceña, P. Vermeulin, P. Archirel, and G. Berthier, *Int. J. Quantum Chem.* **20**, 1285 (1981).
- [107] R. Bartlett, *J. Chem. Phys.* **86**, 887 (1987).
- [108] M. Gordon and D. Truhlar, *Theor. Chim. Acta.* **71**, 1 (1987).
- [109] G. Heard, C. Marsden, and G. Scuseria, *J. Phys. Chem.* **96**, 4359 (1992).
- [110] C. Sosa, C. Lee, G. Fitzgerald, and R. Eades, *Chem. Phys. Lett.* **211**, 265 (1993).
- [111] P.C. Hiberty, S. Humbel, C.P. Byrman, and J. H. Van Lenthe, *J. Chem. Phys.* **101**, 5969 (1994).
- [112] J. Pittner, J. Snydke, P. Arsky, and I. Hubac, *J. Mol. Struct. (THEOCHEM)* **547**, 239 (2001).
- [113] L. Rincon and R. Almeida, *J. Phys. Chem. A* **102**, 9244 (1998).
- [114] S. Shaik, D. Danovich, W. Wu, and P.C. Hiberty, *Nat. Chem.* **1**, 443 (2009).
- [115] P. Jurecka, J. Spöner, J. Cerny, and P. Hobza, *Phys. Chem. Chem. Phys.* **8**, 1985 (2006).
- [116] J. Rezac, J. Fanfrlik, D. R. Salahub, and P. Hobza, *Collect. Czechoslov Chem. Commun.* **73**, 1261 (2008).
- [117] A. Savin, B. Silvi, and F. Colonna, *Canad. J. Chem.* **74**, 1088 (1996).
- [118] X. Krokidis, V. Goncalves, A. Savin, and B. Silvi, *J. Phys. Chem. A* **102**, 5065 (1998).

- [119] X. Krokidis, R. Vuilleumier, D. Borgis, and B. Silvi, *Mol. Phys.* **96**, 265 (1999).
- [120] F. Fuster and B. Silvi, *Theor. Chem. Acc.* **104**, 13 (2000).
- [121] F. Fuster and B. Silvi, *Chem. Phys.* **252**, 279 (2000).
- [122] F. Fuster, B. Silvi, S. Berski, and Z. Latajka, *J. Mol. Struct.* **555**, 75 (2000).
- [123] M.E. Alikhani and B. Silvi, *Phys. Chem. Chem. Phys.* **5**, 2494 (2003).
- [124] B. Silvi, and H. Ratajczak, *Phys. Chem. Chem. Phys.* **18**, 27442 (2016).
- [125] L.E. Seijas, A. Lunar, L. Rincon, and R. Almeida, *J. Comput. Methods Sci. Eng.* **17**, 5 (2017).
- [126] R.L. Jaffe and G.D. Smith, *J. Chem. Phys.* **105**, 2780 (1996).
- [127] P. Hobza, H.L. Selzle, and E.W. Schlag, *J. Phys. Chem.* **100**, 18790 (1996).
- [128] S. Tsuzuki, T. Uchimaru, K. Matsumura, M. Mikami, and K. Tanabe, *Chem. Phys. Lett.* **319**, 547 (2000).
- [129] S. Tsuzuki, K. Honda, T. Uchimaru, M. Mikami, and K. Tanabe, *J. Am. Chem. Soc.* **124**, 104 (2002).
- [130] M.O. Sinnokrot, E.F. Valeev, and C.D. Sherrill, *J. Amer. Chem. Soc.* **124**, 10887 (2002).
- [131] M.O. Sinnokrot and C.D. Sherrill, *J. Phys. Chem. A* **108**, 10200 (2004).
- [132] Y.C. Park and J.S. Lee, *J. Phys. Chem. A* **110**, 5091 (2006).
- [133] R.A. DiStasio, G. von Helden, R.P. Steele, and M. Head-Gordon, *Chem. Phys. Lett.* **437**, 277 (2007).
- [134] O. Bludsky, M. Rubes, P. Soldan, and P. Nachtigall, *J. Chem. Phys.* **128**, 114102 (2008).
- [135] A. Puzder, M. Dion, and D.C. Langreth, *J. Chem. Phys.* **124**, 164105 (2006).